Structure of Wind Field and Variations of Vorticity in a Summer Situation[1]

By C. W. NEWTON, University of Chicago and University of Stockholm,
and J. E. CARSON, University of Chicago[2]

(Manuscript received 7 February 1953)

Abstract

An analysis of the observed wind field at 300 mb is shown for a period when iterative shear-line formations occurred. Each was preceded by the injection of a localized wind maximum into lower latitudes, southwesterly winds subsequently increasing east of the trough line, but not by advection of high winds around the southern end of the trough.

Series of cross sections at different times illustrate the wind variations as the localized jets move through them. These indicate that the local wind maxima at 300 mb reflect similar variations through a deep layer and thus are not due to vertical undulations in the height of the jet stream.

During a time of relatively steady state, changes of vorticity are examined in the region east of the trough, where the jet is weak in lower latitudes and increases in speed downstream. Locally large individual increases of absolute vorticity (of the order of the value of the Coriolis parameter in 12—24 hr) in the upper troposphere are accounted for by the conversion of vertical shear into vorticity about a vertical axis, through differential vertical motions in an indirect solenoidal sense. A simultaneous increase in vertical shear is accounted for by horizontal circulations in a direct solenoidal sense. Considering the trough as a whole, there was weak subsidence in the upper troposphere, with maximum descending motions near the jet stream.

Introduction. — Most synoptic studies of the role of the jet stream in the behaviour of the atmosphere have involved situations in the colder months of the year. This is natural since the jet and the frequently associated extratropical cyclones (RIEHL, 24) are most strongly developed then. A disadvantage of studying the wind field in winter is that direct observations are usually lacking over large regions, because of cloudiness and the instrumental difficulties involved in observing very strong winds.

Partly for this reason, the writers have undertaken an investigation of the structure of the wind field using summer data. In addition to the increased observational data in summer, lower wind speeds make it possible to study the discrete features of the wind field, since these move slowly and therefore remain under observation longer over a network such as that of the United States.

Another reason for looking into summer situations is the possibility simply of changing the point of view from which the investigation is undertaken. For example one might wish to examine the behaviour of specific types of flow patterns observed both in winter, when pronounced frontal surfaces may extend upward through most of the depth of the tropo-

[1] Work performed under a contract between the Office of Naval Research and the University of Chicago.

[2] Present affiliation: Department of Meteorology, Rutgers University, New Brunswick, New Jersey. Participated mainly in earlier phases of work.

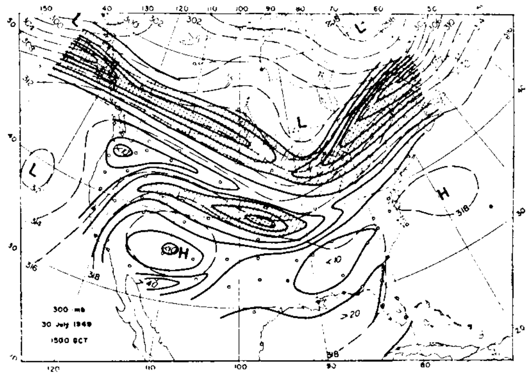

Fig. 1 a. 300-mb chart, 1500 GCT 30 July 1949.

Fig. 1: 300-mb charts from 1500 GCT 30 July to 1500 GCT 5 August 1949. Solid lines, isotachs at 30,000 ft, interval 10 knots; hatched where wind speed is over 50 knots, cross-hatched over 70 knots. In regions of low wind speeds, values indicated by inequality signs and slanted figures. Locations of direct wind observations at 30,000 ft indicated by small circles. Thin long-dashed lines are contours of 300-mb surface (hundreds of ft); short heavy dashes indicate location of shear line where wind speeds are near zero. Note that charts shown for this series are sometimes 12 and sometimes 24 hr apart.

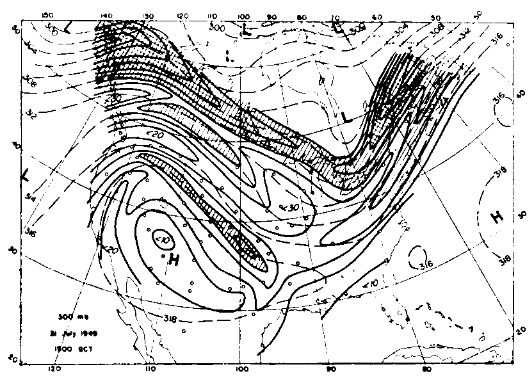

Fig. 1 b. 300-mb chart, 1500 GCT 31 July 1949.

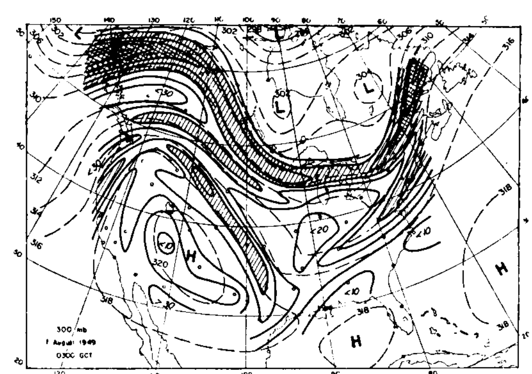

Fig. 1 c. 300-mb chart, 0300 GCT 1 August 1949.

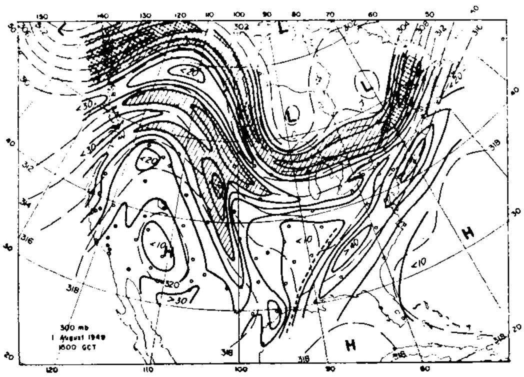

Fig. 1 d. 300-mb chart, 1500 GCT 1 August 1949.

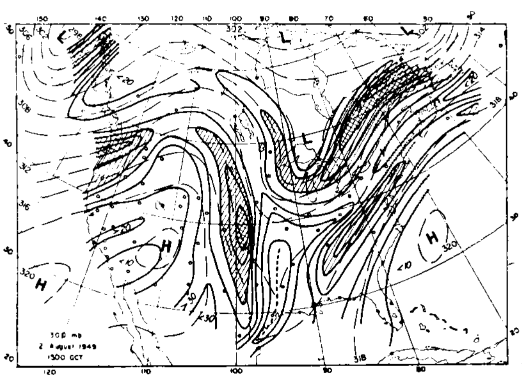

Fig. 1 e. 300-mb chart, 1500 GCT 2 August 1949.

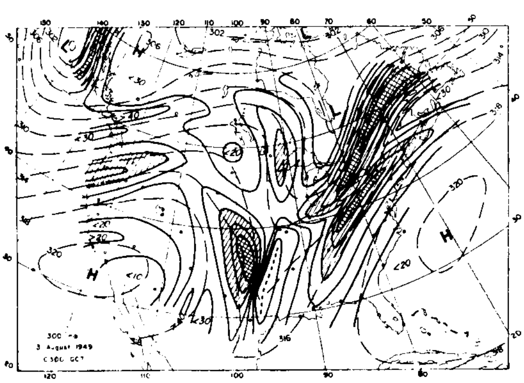

Fig. 1 f. 300-mb chart, 0300 GCT 3 August 1949.

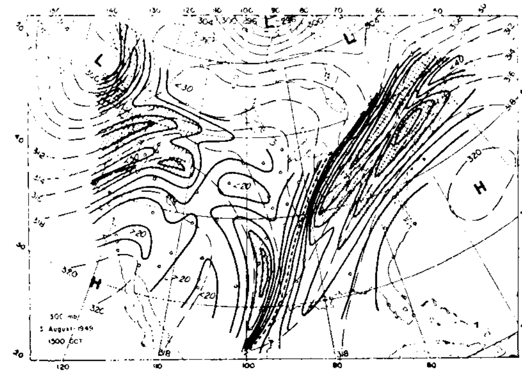

Fig. 1 g. 300-mb chart, 1500 GCT 3 August 1949.

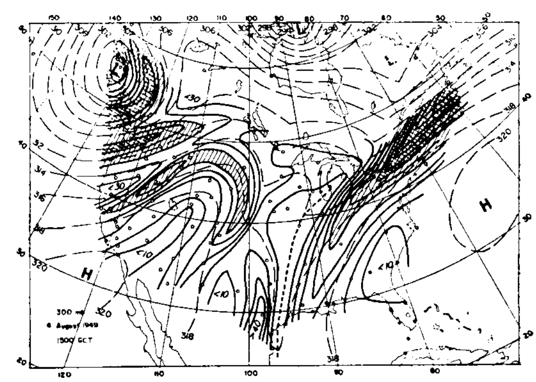

Fig. 1 h. 300-mb chart, 1500 GCT 4 August 1949.

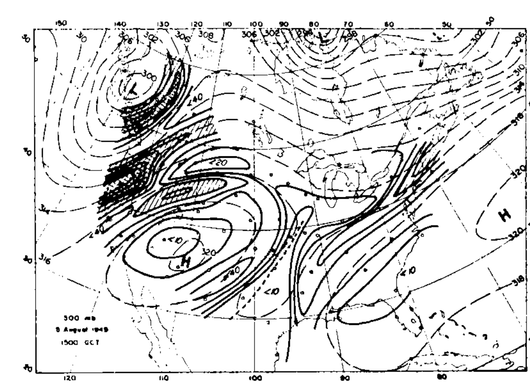

Fig. 1 i. 300-mb chart, 1500 GCT 5 August 1949.

sphere, and in summer, when such fronts might be shallow and far below the level of maximum winds.

One type of flow pattern whose character in summer and winter might be profitably compared is the shear line frequently found near the tropopause level. HSIEH (12) has described the formation of a shear line in winter, as the result of subsidence of an elongated cold tongue following a strong and deep polar air outbreak. HSIEH accounted for the accompanying concentration of vorticity by a pronounced vertical stretching of the layers of air near the tropopause, and the bringing together of the opposing branches of the jet stream bounding the trough. NEWTON, PHILLIPS, CARSON and BRADBURY (16), in a study of a summer shear line, found that the strong shear was confined almost entirely within a layer 150—200 mb deep enveloping the tropopause, there being no evident connection between the large changes of the flow pattern in this layer and the lower tropospheric flow.

Potential absolute vorticity charts for the latter case suggested that the local increases in vorticity observed in the shear-line region were not entirely explainable on the basis of conservation of the vertical component of potential absolute vorticity, $(f + \zeta)/\,\Delta p$. It appears worth while to follow up this conclusion by making a more detailed examination of the processes involved in individual changes of vorticity. Since the vorticity relationships involve real rather than geostrophic winds, the wind field is analyzed so far as possible from direct observations.

Analysis — The following discussion concerns mainly the wind analysis at 30,000 ft, using 300-mb contour charts as a base. While these two levels do not generally coincide, more consistent results are obtained by analyzing the details of the wind field at a constant level, than by interpolation of winds at a constant-pressure surface, since higher-level wind data are given only at 5,000-foot intervals in teletype reports. In addition to observations at the time of radiosonde reports, observed winds six hours before and after each constant-pressure chart were utilized; in many cases this procedure effectively doubled the amount of information available near the time of the charts shown.

In analyzing cross sections, observed winds were used in combination with gradient winds computed from *D*-values (deviations from standard atmosphere heights), as described by BELLAMY (1). No cross sections are shown except those with sufficient direct wind observations to guarantee reasonable accuracy. *D*-values in cross sections were corrected using the apparent errors obtained from contour analyses at the 850-, 500-, 300- and 200-mb levels. Analyses in cross sections and at constant-pressure levels were mutually checked, so that the isotachs on cross sections have in some cases been inferred partly from the wind distribution up- and downstream from the cross sections.

Constant-level isotach analyses — Figure 1 shows a series of 30,000-ft isotach charts for the period 30 July—5 August 1949. Strongest winds were found mostly near 40,000 ft, but the sparsity of observed winds and the greater inaccuracy of constant-pressure analyses at that level made a detailed analysis unreliable there. The major features of the wind field were apparently well-reflected in the 30,000-ft level, though there were at times indications of variations at higher levels which did not appear at 30,000 ft (for simplicity this level will henceforth be referred to as 300 mb).

The large-scale circulation pattern was quite similar to that accompanying a summer shear line studied earlier (16). Throughout the period shown, there were two main jet-stream systems over North America, one entering the continent from the Gulf of Alaska, the other from the region south of a low near latitude 38° N in the eastern Pacific (this low moved westward and slightly southward after fig. 1 a). Throughout the series, the "streakiness" of the wind field is very striking. The presence of separate jet streams at different latitudes has been discussed by CRESSMAN (5), PHILLIPS (22), and MURRAY and JOHNSON (13). A recent analysis of temperature-salinity data in the Gulf Stream area by FUGLISTER (8) suggests an analogous multiple current structure in the barocline regions of the oceans.

Prior to the first map, the jet traversing the Gulf of Alaska and southern Canada was almost zonal, except for a trough south of Hudson Bay. The local wind maximum over the central and western United States in fig. 1 a had moved slowly eastward from the California coast in the preceding two days. Although there were insufficient wind observations to determine whether it extended further east as a definable jet stream, those available as well as continuity indicated a strong decrease in strength downstream as shown.

Each of the jet-stream systems is composed of a chain of discrete well-defined local wind-maxima or "jet streaks"[3], with pronounced velocity gradients along streamlines. These localized wind maxima were first discussed by GUSTAFSON *and collaborators* (9), who noted that they tend to move along with certain synoptic features such as troughs and ridges, at speeds much slower than the strongest winds in the upper troposphere. RIEHL *and collaborators* (25) have discussed in detail the implications of such a velocity distribution for forecasting.

Early in the series, a pronounced deepening occurred in the Gulf of Alaska, continuing until after the time of the last map shown. There ensued a marked amplification of the ridge over western Canada and a deepening of the trough south of Hudson Bay. This deepening was at first rather small in the northern jet-stream system, while a strong deepening was observed in the southern wind system. On the other hand, there was apparently little change in the southern wind system further west over the Pacific Ocean. This suggests that the observed changes might have resulted from some kind of interaction between the northern and southern wind systems.

After the ridge intensified over western North America, there was a pronounced clockwise turning of the jet streak over the west central United States, so that it acquired a more northerly direction. It was proposed in an earlier paper (16) that the strong height rises in the northern part of the ridge, following the deepening upstream in the northern wind system, results in a weakening of the height gradient across the southern jet. As a consequence, the excessive Coriolis force acting on the southern jet results in an increased anticyclonic curvature east of the ridge and a clockwise turning of the winds there.

As the southernmost jet streak changed direction, the maximum wind speed also increased east of the ridge (see figs. 1 b—1 f). Wind observations indicate that increased advection of momentum through the ridge was not entirely responsible for this; it seems likely that the mechanism of wind acceleration downstream from sharp ridges, described by BJERKNES (3), was important in this case. The critical conditions he derived ($r_{min} = 4\,v_g/f$; $v = 2\,v_g$) were approximately satisfied.

Following the turning of the jet streak, a trough with weak shear-line characteristics was observed to form (fig. 1 d), and a southwesterly jet appeared east of the trough line. It is important to note that this jet intensified *in situ*, rather than by advection of high wind speeds around the southern end of the trough. Note that the isotachs move upstream with time in this region (figs. 1 b to 1 f). The shear line evidently formed as a consequence of the injection of the northerly jet streak into lower latitudes.[4]

When the trough first deepened (figs. 1 c—1 d), the greatest horizontal shear and vorticity were found not at the trough line itself, but on the cyclonic flank of the jet streak some distance west. Between 1500 GCT 1 August and 1500 GCT 2 August (figs. 1 d—1 e) the weak winds in the stagnant region between the jets gradually backed and increased in strength, a new shear line forming adjacent to the northerly jet. This reached greatest development near 1500 GCT 3 August (fig. 1 g), when the 34,000-ft winds at Fort Worth and Shreveport, 350 km apart, indicated an average horizontal shear of 17 m sec^{-1} per 100 km (absolute vorticity 3.1 times the Coriolis parameter at that latitude). After 0300 GCT 1 August, the jet streak over the eastern slope of the Rocky Mountains moved southward, first intensifying, then finally weakening and moving entirely out of the field of observation, into Mexico. During this time, the southwesterly current east of the trough first increased, then decreased in speed, at lower latitudes. Between 1500 GCT 1 August and 1500 GCT 3 August, a distinct

[3] By analogy to the "streak lines" showing trajectories of fast-moving tracer particles in photographs of hydrodynamics experiments.

[4] This conclusion is drawn from the apparently direct association of events locally. In the three days preceding 3 August, the Atlantic subtropical high moved about 20° longitude westward. During the first week of August, there was a general westward retrogression of the major troughs and ridges on a hemispheric scale (see NAMIAS and CLAPP (14), CRESSMAN (4)). The deepening in the Gulf of Alaska (fig. 1) and the subsequent formation of the shearline trough are part of this large-scale process.

jet streak (the one furthest southeast in figs. 1 e—1 g) formed east of the trough and intensified as it moved northeastward, apparently moving out over the ocean by 1500 GCT 4 August.

In the northern jet-stream system, the behaviour appears quite normal up until 1500 GCT 1 August (fig. 1 d). The initial increase in amplitude of the Rocky-Mountain ridge was followed by a replacement of the trough near Hudson Bay. By 1500 GCT 2 August (fig. 1 e), the jet crossing southern Alaska had turned sharply to a more southerly orientation and a new ridge built up north of the one observed earlier. By this time, the northern jet stream no longer appeared to be continuous across western Canada. Subsequently, the part of the jet between the ridge and the Hudson-Bay trough gradually decreased in strength, presumably because its source of momentum had been cut off on the upstream side. By 0300 GCT 3 August (fig. 1 f) the trough in the northern jet-stream system began to have the characteristics of a shear line, and 12 hr later (fig. 1 g), after a further weakening of the northerly branch, only that part of the jet east of the Hudson-Bay trough remained in strength.

Up until 0300 GCT 3 August (fig. 1 f), the axis of the southern wind maximum appeared to be continuous, between the jet streak entering the Pacific coast and the one just east of the Rockies. Twelve hours later (fig. 1 g), there was a definite break in this axis. Following this time (fig. 1 h), the jet streak moved eastward from the Pacific coast, curving sharply anticyclonically into a region 400—700 km west of the axis of the earlier jet streak, which now could no longer be considered as part of the same jet-stream system. By 1500 GCT 5 August (fig. 1 i), a new shear line had formed on the cyclonic flank of the new jet now being injected into lower latitudes, winds east of this line slowly backing to a southerly direction. Rapid replacement of shear-line troughs in this manner is quite common, the older shear line often completely disappearing in 12 to 24 hours. After 5 August, the southwesterly jet streams on the west coast increased in strength, while the flow pattern further east over the United States remained relatively steady for some days.

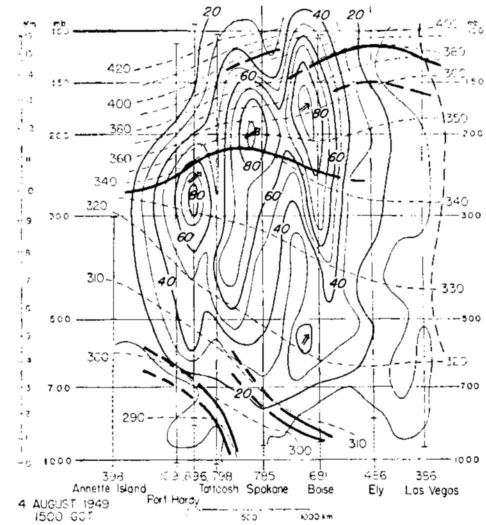

Fig. 3. Vertical cross section from Annette Island, Alaska, to Las Vegas, Nevada, at 1500 GCT 4 August 1949. Solid lines, isotachs (knots) of total wind speed, dashed for zero wind speed. Wind blows into page. Direction of wind indicated by double-shafted arrows near wind maxima (oriented as though north were at top of page). Thin dashed lines, isentropes (deg K); heaviest lines tropopauses and boundaries of stable layers. In all cross sections, pressure scale is logarithmic up to 200 mb, but is contracted to a linear scale above 200 mb.

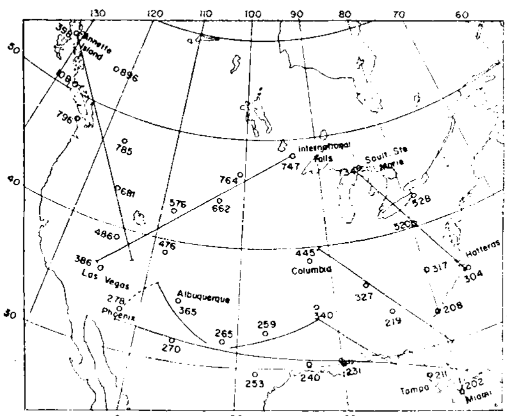

Fig. 2. Locations of cross sections in figs. 3 to 6, with index numbers of radiosonde stations used. Cross sections in fig. 5 varied slightly in location within limits of southernmost pair of lines, so that sections could be oriented normal to 300-mb flow.

Three-dimensional structure of the wind field — Every 12 hours during the period studied, vertical cross sections were analyzed at the locations shown in fig. 2. Figure 3 shows the wind distribution near the Pacific coast,

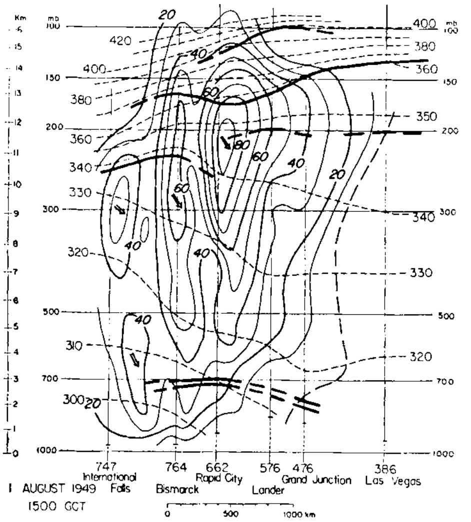

Fig. 4 a. Cross section from Las Vegas, Nevada, to International Falls, Minnesota, at 1500 GCT 1 August 1949.

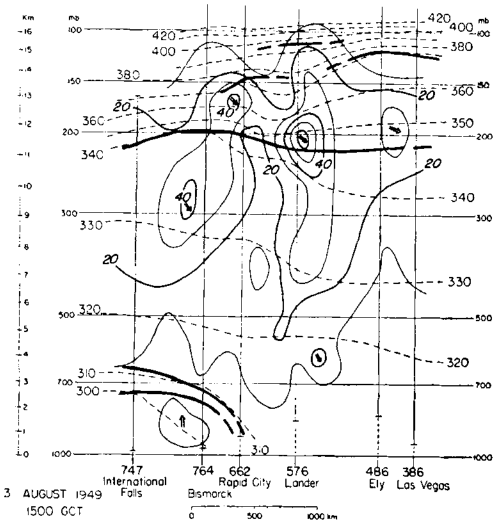

Fig. 4 c. Cross section from Las Vegas to International Falls, 1500 GCT 3 August 1949.

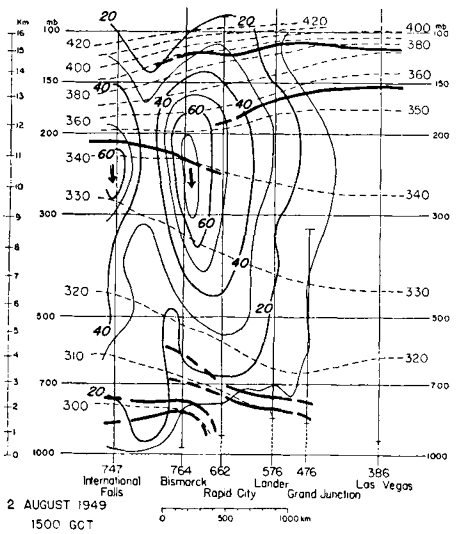

Fig. 4 b. Cross section from Las Vegas to International Falls, 1500 GCT 2 August 1949.

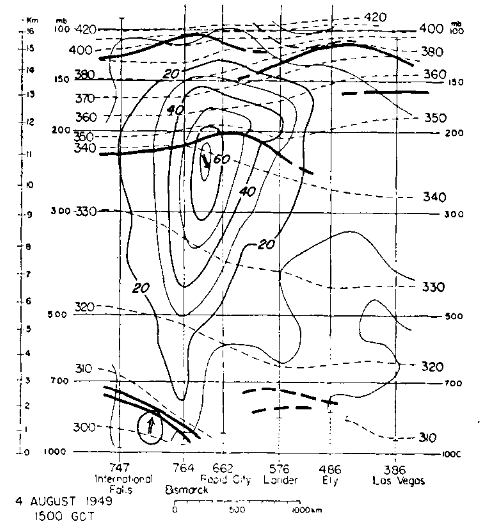

Fig. 4 d. Cross section from Las Vegas to International Falls, 1500 GCT 4 August 1949.

toward the end of the series of fig. 1. The center jet in this figure, which was quite variable in strength at 300 mb (cf. fig. 1), is not a part of the principal jet-stream systems discussed earlier; its role is completely obscure to the writers. Although cross sections were made for this location at 12-hourly intervals throughout the period being studied, the sparsity of wind observations particularly in the northern part made the results quantitatively unreliable much of the time. However, most of the time there was evidence of a complicated wind field similar to that shown in fig. 3. When jets are this close together, it is often impossible to get any indication of their structure (or even of their separate existence)

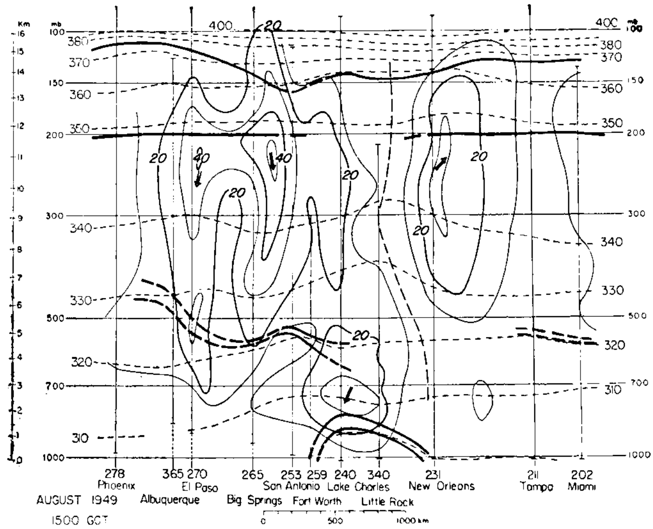

Fig. 5 a. Cross section from Phoenix, Arizona, to Miami, Florida, at 1500 GCT 1 August 1949. Winds with southerly component (indicated by double-shafted arrow) blow into page; with northerly component out of page.

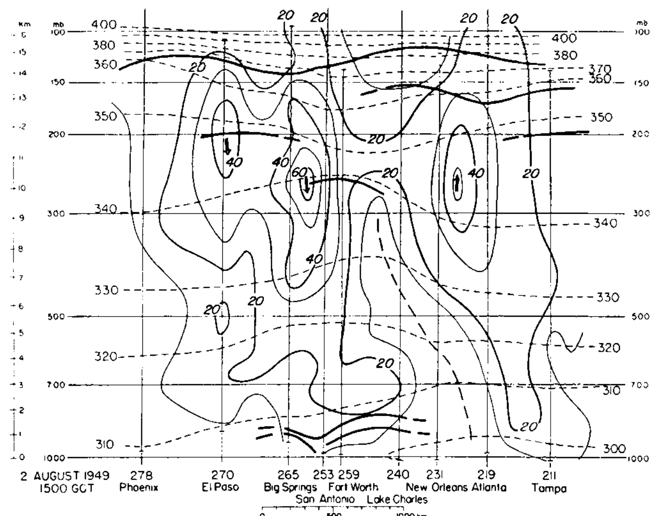

Fig. 5 b. Cross section from Phoenix to Tampa, Florida, 1500 GCT 2 August 1949.

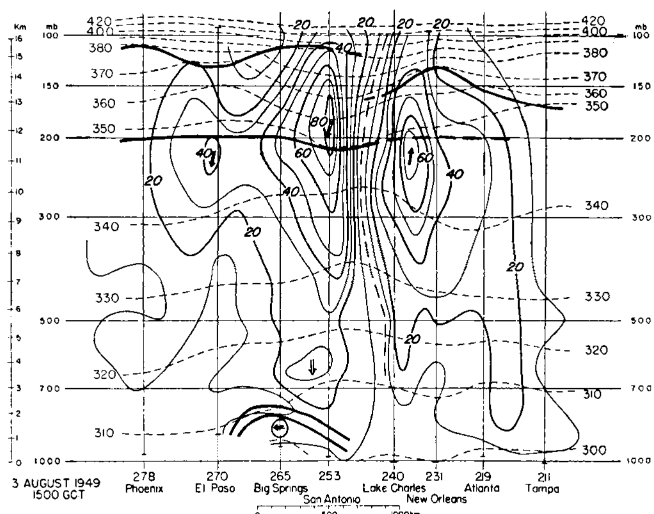

Fig. 5 c. Cross section from Phoenix to Tampa, 1500 GCT 3 August 1949.

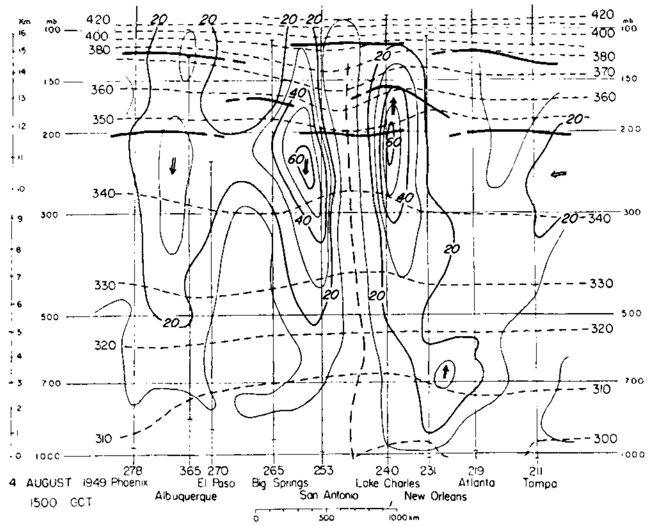

Fig. 5 d. Cross section from Phoenix to Tampa, 1500 GCT 4 August 1949.

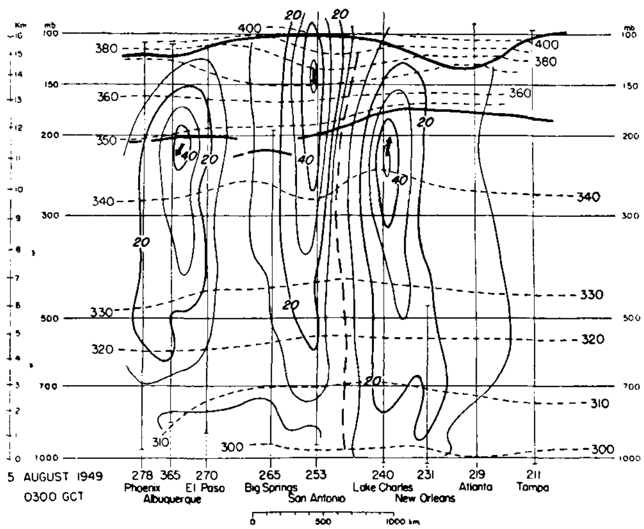

Fig. 5 e. Cross section from Phoenix to Tampa, 0300 GCT 5 August 1949.

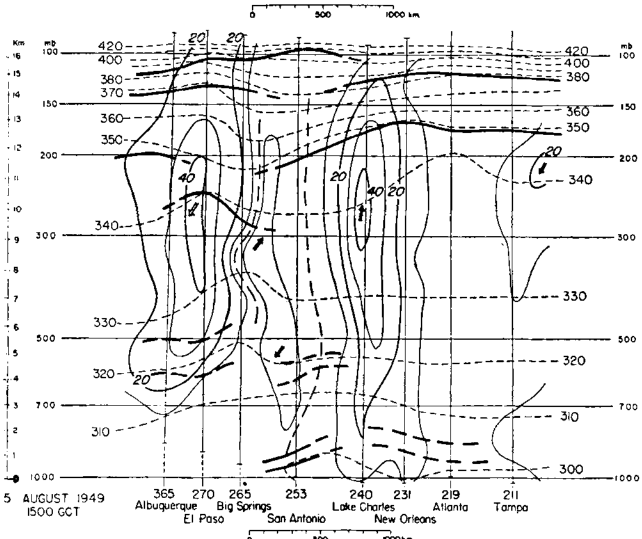

Fig. 5 f. Cross section from Albuquerque, New Mexico, to Tampa, at 1500 GCT 5 August 1949.

from radiosonde observations alone. It is obviously of fundamental importance, in understanding the mechanism of certain types of atmospheric phenomena, e.g. blocking, to know whether there is this type of wind field upstream from the block or whether a splitting of a single jet is involved. In the present case, it is clear that the principal jet streams maintain their separate identities through the region near the west coast where they flow close together.

One might legitimately ask whether the jet streaks observed at 300 mb represent variations of the wind throughout a deep layer of the atmosphere, or whether they can be accounted for largely by vertical undulations of a more uniform jet. To provide the answer to this question a number of vertical cross sections are shown illustrating the local changes of the wind field with time.

Figure 4 shows a series of cross sections normal to the 300-mb flow east of the Rocky-Mountain ridge. The local variations of wind-speed in the right-hand jet (corresponding to the southern jet-stream system) are very striking. At the time of fig. 4 a (cf. fig. 1 d), the center of the 300-mb jet streak was near the location of the cross section. As the jet streak moved south, there was a very marked local decrease in wind speed at all levels until 1500 GCT 3 August (fig. 4 c), when the cross section was near the break between the earlier jet streak and the one involved in the last shear-line formation (see fig. 1 g). By 1500 GCT 4 August (fig. 4 d), the latter jet had moved into the cross section and again a great increase of wind was observed at all levels.

It may be concluded that the major features of the 300-mb wind field in fig. 1 are representative of concomitant variations through a deep layer of the upper troposphere and lower stratosphere. This is not necessarily always the case,[5] although experience with a variety of situations indicates that the major wind variations at a single level in the higher troposphere cannot usually be explained only on the basis of vertical undulations of the jet without significant variations at the level of maximum wind. In the lower troposphere (e.g 500—700 mb), pronounced local wind maxima are frequently observed which are not connected with similar features near the tropopause level.

Wind variations near latitude 30° — A series of cross sections at about 30° latitude, near the southern border of the United States, is shown in fig. 5. From 1500 GCT 1 August to 0300 GCT 5 August, these show (between Big Springs and San Antonio) the local variations in wind strength as the large jet streak east of the Rockies passes southward through this location (cf. figs. 1 d—1 h)[6]. The changes on the west side are closely followed by like variations in strength of the jet east of the trough line. This suggests that the air particles east of the trough are accelerated in response to changes in the pressure field brought about by adjustment to the wind field west of the trough.

By 1500 GCT 5 August (fig. 5 f), the earlier northerly jet streak was no longer in evidence at the latitude of the cross section, and the winds further west had intensified locally as the new jet streak moved into this region. This intensification continued further for 12—24 hours. At 1500 GCT 5 August (cf. fig. 1 i), there was a broad region of stagnant air between the old and the newly-forming shear lines. After this time, the winds in this region gradually backed to a southerly direction and increased in speed, essentially repeating the process which had occurred earlier between 1500 GCT 1 August and 1500 GCT 2 August (figs. 1 d—1 e). The local readjustment of the mass field during formation of the shear lines may be seen from the changes in distribution of

[5] Lt. W. E. Hubert, in studying the wind variations over the British Isles during a period of relatively straight westerly flow, has found that the elevation of the jet varies locally as much as 200 mb in 12—18 hr. (See report elsewhere in this issue.)

[6] It might be pointed out that the apparent discrepancies between analyzed wind and temperature fields in the cross sections are not all real. For example, at San Antonio in fig. 5 c there is strong vertical shear between 500 and 200 mb, connected with a rather weak horizontal potential temperature gradient. For curved flow, if the variation of trajectory curvature with height is neglected, the thermal wind equation is

$$\frac{\partial v}{\partial z} = - \frac{g}{\left(f + \frac{2v}{r}\right) T} \frac{\partial T}{\partial n},$$

where r is positive for cyclonic curvature. At 300 mb in the example cited above, $r = 1{,}500$ km anticyclonic, $v = 30$ m sec.$^{-1}$ and $2v/r = -0.4 \times 10^{-4}$ sec^{-1} or half the value of the Coriolis parameter. Thus the computed *geostrophic* wind shear would give only half the actual vertical shear.

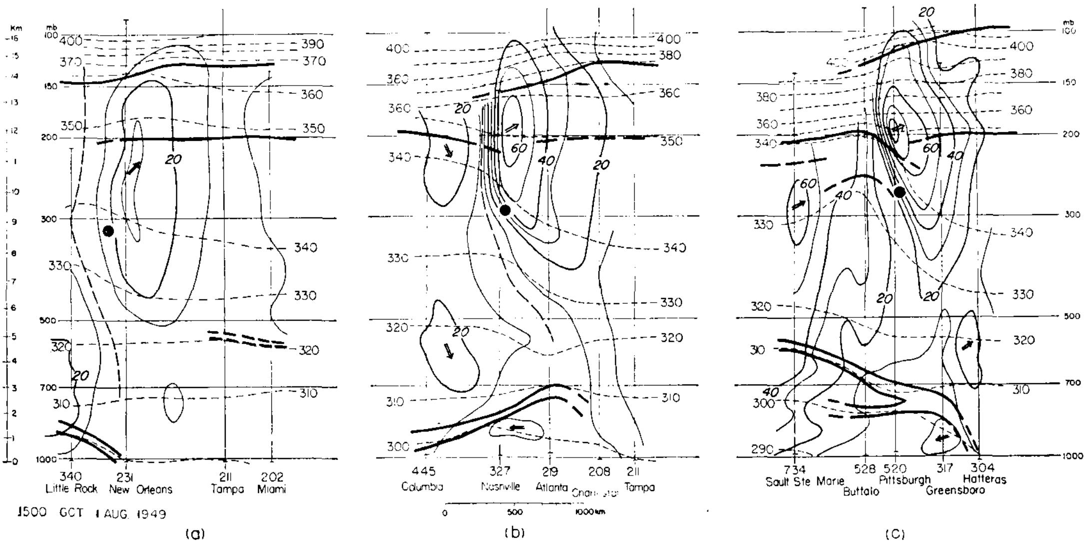

Fig. 6. Cross sections through southwesterly jet east of shear line at 1500 GCT 1 August 1949, (a) Little Rock, Arkansas, to Miami, Florida; (b) 550 km downstream, Columbia, Missouri, to point NE of Tampa, Florida; (c) 750 km further downstream, Sault Ste. Marie, Michigan, to Hatteras, North Carolina. Wind blows into page. Heavy dots indicate regions for which computations in text are made.

isentropes (particularly 340 and 350 Θ), e.g. in the central part of figs. 5 a to 5 c and on the left or west side of figs. 5 d to 5 f.

Throughout this series of cross sections, there was near latitude 30° a second weaker northerly wind maximum, west of the principal jet discussed above. This appeared only weakly at 300 mb until the advection of the second pronounced jet streak into this region on 4 August. Observations are insufficient to make any very definite statements about this feature of the wind field; however, it appears certain that before this time there was no connection between the low- and higher-latitude wind maxima in this region.

Structure of jet east of shear line — Figure 6 shows three cross sections through the jet east of the trough, at 1500 GCT 1 August. A comparison of these, about 650 km apart, shows a strong increase in wind strength toward the northeast. Cross sections at other times indicated the same sort of changes along the jet, although there were of course time-variations in wind speed at the three locations. As a first approximation, it seems permissible to discuss certain features of the wind field as though steady state existed. Thus it may be said that for the most part air particles passing through the southernmost cross section underwent a marked acceleration in moving toward the northeast, during the whole period. This acceleration was most pronounced near the 200-mb level.

Vorticity variations — Obviously such a complicated wind field as that shown in fig. 1 must be connected with great variations in absolute vorticity,[7] along as well as normal to the streamlines. This is particularly true in the regions up- and downstream from individual jet streaks, and on the cyclonic-shear side. Since the jet streaks move with speeds considerably less than the maximum winds, and greater than the speed of the winds in the stagnant regions between jets, this implies that individual air particles passing through the jet streaks must undergo large changes in absolute vorticity. If the circulation about a vertical axis is conserved, an increase in absolute vorticity must be accompanied by horizontal convergence and vertical stretching of individual air columns. It is well known, however, that regions of highest absolute vorticity

[7] Hereafter the unqualified terms vorticity, potential absolute vorticity, etc., refer to the vorticity in a horizontal plane or pressure surface, or the component of the vorticity about a vertical axis.

are more likely to be stable than unstable, so that at least near the level of maximum wind, individual changes of vorticity cannot be accounted for by a horizontal divergence process.

Since the closest approach to steady-state flow is found in the southwesterly jet east of the shear line trough, it is most convenient to look there in order to examine the factors which tend to modify the vorticity. In fig. 6, the pronounced increase in slope of the higher-troposphere isentropes downstream suggests that vertical motions must be important in contributing to the vorticity changes.

The equation for the component of absolute vorticity $(f + \zeta)$ about a vertical axis may be written

$$\frac{d}{dt}(f+\zeta) = -(f+\zeta)\,D_{xy} + \left(\frac{\partial w}{\partial y}\frac{\partial u}{\partial z} + \frac{\partial w}{\partial x}\frac{\partial v}{\partial z}\right) + \left(\frac{\partial \alpha}{\partial y}\frac{\partial p}{\partial x} - \frac{\partial \alpha}{\partial x}\frac{\partial p}{\partial y}\right) + \left(e\frac{\partial w}{\partial y} + w\frac{\partial e}{\partial y}\right) + \text{friction}, \quad (1)$$

where $D_{xy} = (\partial u/\partial x + \partial v/\partial y)$ is the horizontal divergence, $e = 2\,\omega\cos\varphi$ the component of the earth's vorticity about an axis pointed north, and the other symbols have their usual meanings. The terms involving e are insignificant, while the solenoidal terms vanish if a constant-pressure surface is considered (in that case the vertical velocity w must be measured with respect to the pressure surface). The effect of frictional torques is unknown. Aside from this, *the only terms available to account for the changes in* potential *absolute vorticity are those involving the vertical wind shear combined with differential vertical motions.*

If the x-axis is placed along a streamline, the contribution from these terms may be evaluated from the single term $(\partial w/\partial y)\,(\partial u/\partial z)$ if, as in the present case, the wind direction does not change too rapidly with height. Using a mean wind speed of 15 m sec^{-1} in the cyclonic shear zone, the cross-stream gradient of vertical motion computed from the change in tilt of isentropes downstream (e.g. the isentrope 340 A changes tilt from 1/500 in fig. 6 a to more than 1/100 in fig. 6 c) is about 1 cm sec^{-1} (100 km)$^{-1}$. In fig. 6 b, the strongest vertical shear, coinciding approximately with the 337 A isentrope, is about 20 m sec^{-1} per km. Using these values,

$$\frac{\partial w}{\partial y}\frac{\partial u}{\partial z} = 2 \times 10^{-9}\ \text{sec}^{-2},$$

of the same order as the divergence term in cases with strong vertical motions (see, e.g., PALMÉN (17)).

From fig. 6 a to fig. 6 c, the maximum absolute vorticity (in region marked by heavy dot) increases from about 10^{-4} to 3×10^{-4} sec^{-1}. Assuming a mean wind speed of 15 m sec^{-1} between the two sections in the region of highest vorticity, the individual rate of change of vorticity is about 2×10^{-4} sec^{-1} per 24 hr, or 2.3×10^{-9} sec^{-2}. Comparing this value with that obtained above, we see that the differential-vertical-motion term can account for most of the observed change in absolute vorticity. In the region for which the above computations were made (between 330 and 340 A potential temperature), there was little or no divergence. Above the level of strongest wind (e.g. $\Theta = 390$ A), there is evidence of a weaker vertical motion gradient opposite to that observed in the troposphere. Here, since the wind decreases with height, the differential-vertical-motion term also contributes to an increase of vorticity downstream.

Between the levels of strongest vertical motion, there was pronounced horizontal divergence[8]. As $(\partial w/\partial y)\,(\partial u/\partial z)$ must obviously be rather unimportant in this region, there is no apparent way to account for the observed changes in vorticity, since the divergence indicates a decrease rather than an increase. It might of course be hypothesized that some sort of frictional torques come into play here, in bringing about an adjustment of the vorticity field with that at higher and lower levels. Heavy clear-air turbulence is often encountered in this region (see, e.g., BERGGREN (2)). However, it would be best to avoid conjecture until more is known about the actual distribution of wind and temperature in this region.[9]

[8] The total divergence judged from changes in vertical packing of isentropes, e.g. 340 to 360 A, in fig. 6, is very much exaggerated, since in those levels the stability decreased with time in the sections furthest downstream.

[9] Near the level of maximum wind, the *potential* absolute vorticity may be regarded as essentially constant on the left side of the region of highest absolute vorticity,

It is safe to conclude that, at least in a significant part of the jet-stream region, the observed changes in absolute vorticity can be accounted for by differential vertical motions combined with the vertical wind shear. Furthermore the above example shows that *the differential-vertical-motion terms usually neglected in the vorticity equation are capable of creating or destroying vorticity at the rate of* 10^{-4} sec^{-1} *(the value of the Coriolis parameter in middle latitudes) in 12 to 24 hours.* This is roughly *ten times* the size of the df/dt (or βv) term, in the example considered above. It must be realized, of course, that the vertical-motion term is this large in a restricted region only, while the βv term becomes important when integrated over extensive regions. SHERMAN (28) has shown that the vertical-motion terms are of the same order of magnitude as the βv term, for middle-latitude disturbances of wavelength around 4,500 km.

Generation of vertical wind shear — According to fig. 6 a, the cross section furthest upstream, there was initially very little vertical wind shear from which vorticity could be derived. It is therefore necessary to account for the increase in vertical shear as well as the vorticity, as the air particles moved downstream. Since (discounting friction) the only way in which axial acceleration can occur in the free atmosphere is through a pressure force acting in the direction of motion, to increase the vertical shear there must be a greater cross-isobar flow toward lower pressure in the upper than in the lower levels; in other words the quasihorizontal branches of the circulation must be in a direct solenoidal sense.[10]

The vorticity equation for the x—z plane may be written (x-axis eastward)

$$\frac{d\sigma}{dt} = -(\sigma + e)\, D_{xz} + \frac{\partial v}{\partial z}\left(f - \frac{\partial u}{\partial y}\right) + \frac{\partial v}{\partial x}\frac{\partial w}{\partial y} + \frac{\partial}{\partial x}\left(\alpha\frac{\partial p}{\partial z}\right) - \frac{\partial}{\partial z}\left(\alpha\frac{\partial p}{\partial x}\right) + \text{friction} \ldots \quad (2)$$

with a similar equation for the y—z plane. Here $\sigma = (\partial u/\partial z - \partial w/\partial x) \approx \partial u/\partial z$ is the component of vorticity about the y-axis and $D_{xz} = (\partial u/\partial x + \partial w/\partial z)$ the divergence in the x—z plane. If the small term in e, the insignificant third term and the frictional torques are neglected, and the hydrostatic and geostrophic relationships substituted in the solenoidal terms, this becomes

$$\frac{d\sigma}{dt} \approx -\sigma\, D_{xz} + f\left(\frac{\partial v}{\partial z} - \frac{\partial v_g}{\partial z}\right) - \frac{\partial v}{\partial z}\frac{\partial u}{\partial y}. \quad (3)$$

This equation is closely analogous to the corresponding equation (1) for the component of vorticity about a vertical axis. The first term on the right states that divergence in the x—z plane tends to decrease the existing vertical wind shear in that plane. The term

$$f\left(\frac{\partial v}{\partial z} - \frac{\partial v_g}{\partial z}\right) = \frac{\partial}{\partial z}(fv - fv_g) = \frac{\partial}{\partial z}\left(\frac{du}{dt}\right)$$

corresponds to the vertical gradient of the horizontal acceleration due to flow of air across pressure contours, and the term $-(\partial v/\partial z)(\partial u/\partial y)$ represents a readjustment of the existing wind field by differential horizontal advection at different levels.

It is important to realize that the terms $(\partial w/\partial y)(\partial u/\partial z)$ in equation (1) and $(\partial v/\partial z)(\partial u/\partial y)$ in equation (3), *each of which makes use of the vorticity about one axis to generate vorticity about an orthogonal axis, do not in themselves change the amount of vorticity about the original axes.* This follows from the advective nature of these terms, since advection without deformation is incapable of changing the gradient of the quantity (in this case, wind speed) being advected. Thus for instance the creation of vorticity about a vertical axis from the vertical wind shear does not necessarily mean that the vertical shear is consumed in the process (see fig. 7). If potential temperature is conserved, each of the terms discussed above, taken individually, implies a nonconservatism of the total three-dimensional absolute vorticity (ERTEL (6)).

If the x-axis is taken along an isotherm, $\partial v_g/\partial z = 0$ and

$$\frac{d\sigma}{dt} \approx -\sigma D_{xz} + \zeta_s \frac{\partial v}{\partial z}, \quad (4)$$

where $\zeta_s = (f - \partial u/\partial y)$ is the "shearing vorticity", or the absolute vorticity neglecting

and on the right side of the band of minimum absolute vorticity flanking the jet stream, with a strong gradient of potential absolute vorticity in between. PLATZMAN (23) has investigated the consequences of such a vorticity distribution for the motion of atmospheric disturbances.

[10] For an interesting discussion of the transversal circulation about the axis of an atmospheric current, with particular regard to the jet stream associated with large-scale wave patterns, the reader is referred to an article by VAN MIEGHEM (30).

curvature (this is strictly true only if isotherms and streamlines are parallel).

Equation (4) may be applied in the vicinity of the jet east of the shear line at 1500 GCT 1 August, where the angle between isotherms

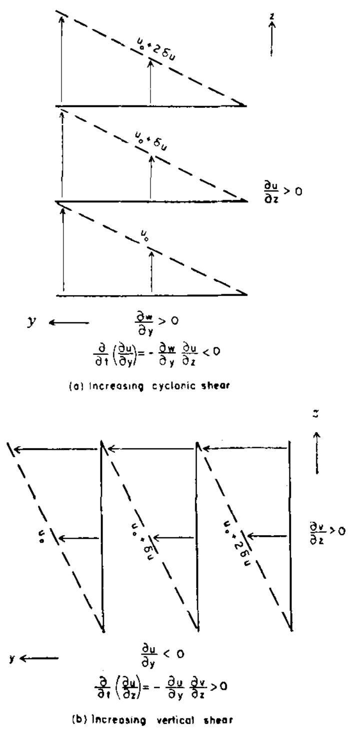

Fig. 7. Schematic illustration of terms in vorticity relationships involving readjustment of the existing wind field. Heavy solid lines represent initial isotachs (wind blowing into page; backing with height in fig. 7 b); dashed lines the same isotachs at a later time. The vertical velocity field (fig. 7 a) does not by itself change the initial vertical shear, nor the field in fig. 7 b the initial horizontal shear, though these fields contribute to changes of circulation in the orthogonal xy- and xz-planes respectively.

and contours is small in the layer 500—300 mb. In the cyclonic-shear zone between figs. 6 a and 6 b, where the vertical shear increased most rapidly downstream, the total cross-isotherm component of the vertical shear is estimated (from wind analyses at 300 and 500 mb) to be about 5 knots in that layer. The few direct wind observations in this region indicate that the backing of wind with height was most pronounced in the region of strongest vertical shear. If the above amount of cross-isotherm shear is assumed to be concentrated in the 1-km-deep layer of greatest vertical shear (between 335 and 340 A potential temperature in figs. 6 a—6 b), this gives $\partial v/\partial z = 2.6 \times 10^{-3}$, while the shearing vorticity has a mean value of around 1.7×10^{-4} sec^{-1}. Then

$$\zeta_s \frac{\partial v}{\partial z} \approx 4.4 \times 10^{-7} \text{ sec}^{-2} = 38 \text{ m sec}^{-1}/\text{km}$$

per day.

A mean wind speed of 25 knots between the two sections in this region, where the total change of vertical shear was 15 m sec^{-1}/km in 300 nautical miles downstream, gives an actual change in shear at the rate of 30 m sec^{-1}/km per day. This agrees well with the above computation, considering the possible inaccuracies of estimate of the quantities involved. Clearly *the term $\zeta_s\, \partial v/\partial z$, involving circulation about the axis of flow in a solenoidal sense, is capable of accounting for large changes in the vertical wind shear*, of the magnitude required to account for the observed wind distribution.

It is essential to realize that the net effect of this term, integrated for instance along the vertical through a deep layer, depends upon the particular distributions of ζ_s and $\partial v/\partial z$. If large values of one of these quantities are associated with small values of the other, the total change in vertical shear must necessarily be smaller than if large values of both quantities are found together.

The nonconservative term in the equation for vertical shear is proportional to the shearing vorticity. Large changes are therefore to be expected from this term on the cyclonic-shear side of the jet, while on the anticyclonic-shear side its contribution is relatively weak. Given a proper combination of vertical motions and cross-contour flow, the vertical and horizontal shears increase simultaneously. Figure 8 shows the combined fields of fig. 7 and the resulting deformation of an initial isotach distribution. This represents schematically the type of motions observed in the cyclonic-shear zone from fig. 6 a to fig. 6 c, in the troposphere. The readjustment indicated here does not include the Coriolis acceleration, which would contribute directly to a further increase in the vertical shear, and indirectly to increasing the horizontal shear.

The above discussion does not consider the effect of divergence in the x—z plane. In this case, vertical motions are small and the first and last terms of the continuity equation

$$\frac{1}{\varrho}\frac{d\varrho}{dt} + \left(\frac{\partial u}{\partial x} + \frac{\partial v}{\partial y} + \frac{\partial w}{\partial z}\right) = 0$$

are of the order 5 to 10×10^{-7} sec^{-1}, while the other terms are an order of magnitude larger.

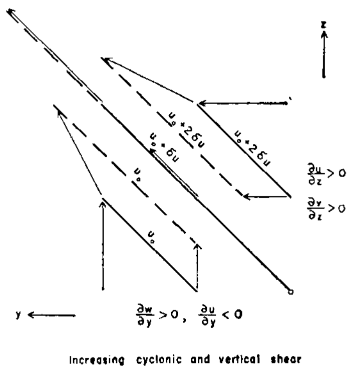

Fig. 8. Combination of fields in fig. 7 (scale of vertical velocities exaggerated roughly 500 times with respect to horizontal components).

Thus $D_{xz} \approx \partial u/\partial x \approx -\partial v/\partial y$, and divergence in the vertical plane corresponds to "confluence" in the x—y plane with dilatation along the x-axis.

On the cyclonic side of the jet in the region discussed above, $-\partial v/\partial y$ is at most 2 m sec^{-1} (100 km)$^{-1}$. Assuming a mean vertical shear of 10 m sec^{-1}/km between 500 and 300 mb, the divergence term $-\sigma D_{xz}$ of equation (4) is then -1.4×10^{-7} sec^{-2}, the same order of magnitude but of opposite sign and much smaller than $\zeta_s \partial v/\partial z$ for the same layer. Here again, the detailed distribution of σ and D_{xz} are important.

The computations in this and the preceding section give results satisfactory within the limits of observation and analysis, and demonstrate that in principle there is no difficulty in accounting for the generation of strong vertical shear and high values of absolute vorticity. This is so at least in the regions above and below the level of maximum wind. However, near that level, the processes involved in generation of vorticity remain in question.

Larger-scale advective processes and vertical motions — The reason why the instability in an upper wave development should express itself sometimes through the formation of a shear line rather than the more common form of sinusoidal trough, is at best vaguely understood. Despite this fact, the type of development described above lends itself to a rather simple discussion of the manner of local adjustment of pressure and wind fields.

As indicated earlier, the shear-line formation was preceded by an injection of a pronounced northerly current into lower latitudes, west of the locale of trough development. The southwesterly current east of the shear line did not become well developed until after this took place, and the very weak flow through the southern part of the trough indicated that advection of momentum into the region east of the trough was of little importance in the development of the jet stream there. Because of this peculiarity of the wind distribution, the shear line presents a simple illustration of the familiar concept of mutual adjustment of velocity and pressure fields (26).

The individual trough developments at 300 mb were accompanied by the slow southeastward movement of cold fronts, distinct at the surface but shallow in vertical extent (generally below 700 mb). Figure 9 shows the surface map at the time of strongest shear-line development (cf. fig. 1 g). As is usual in the case of strongly-developed high-level shear lines, only very weak wave developments took place in the lower frontal systems. The major changes in flow patterns in higher and lower levels were not always clearly connected. For instance,

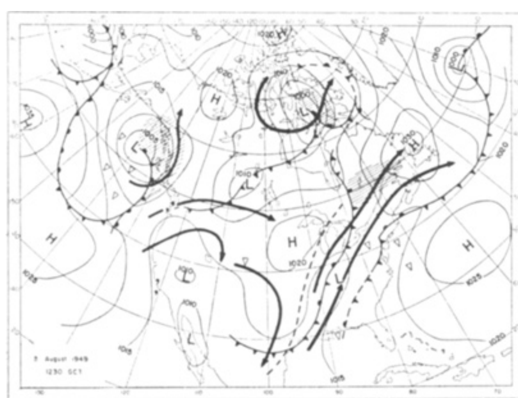

Fig. 9. Sea-level chart at 1230 GCT 3 August 1949. Thin solid lines, isobars; surface fronts indicated by usual symbols, precipitation by hatching and shower symbols. Heavy arrows indicate axes of jet streams at 300 mb. Location of shear line (compare fig. 1 g) indicated by heavy dashed line extending SSW from Great Lakes to Texas.

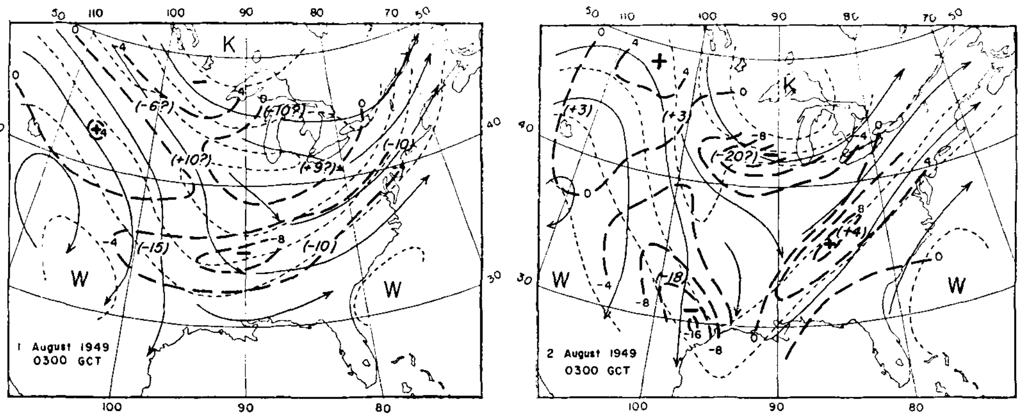

Fig. 10. Mean isotherms (dashed lines, interval 2 C) and mean streamlines (thin arrows) in layer 500—300 mb, (a) 0300 GCT 1 August, (b) 0300 GCT 2 August 1949. Warm and cold regions indicated by W and K Indicated advective temperature change shown by heavy dashed lines (upright numbers); centers of actual loca temperature change by larger slanted numbers in parentheses (units 0.2 C per 12 hr).

although the initial shear-line development in this series occurred behind the connected surface cold front, the last shear line (figs. 1 g —1 h) formed quite far ahead of the nearest surface front (fig. 9, over Rocky Mountains).

Height changes at the 1,000-mb surface were very weak compared with those in higher levels; in fact the predominant part of the 300-mb height changes could in this case be expressed by changes in the relative topography (mean temperature) field in the layer between 500 and 300 mb. In studying the processes in the upper levels it may therefore be regarded as sufficient to examine the adjustment processes in that layer.

Figure 10 shows the mean isotherms and mean streamlines in the 500—300 mb layer at two times during the trough development. West of the trough, both maps indicate strong cold advection where the streamlines cut strongly across the mean isotherms between latitudes 30° and 40°. Cold advection in this region continued up until 3 August when the trough reached maximum development. East of the trough, there was at first cold advection (fig. 10 a) but after 2 August (fig. 10 b) there was warm advection. The indicated advection was most pronounced near the jet streams, and exceeded the value of the actual local temperature change which in general was of like sign.

Thus the adjustment of the contour field at 300 mb could be accounted for chiefly by thermal advective processes, mainly by cold advection below that level following the injection of strong northerly winds into lower latitudes. West of the trough, the lag in adjustment of isotherm and contour orientation behind changes in wind direction clearly indicated that the wind changes were responsible for the height changes in upper levels. Generation of southwesterly winds east of the trough occurred in response to an increased height gradient there following the central deepening, as evidenced by the fact that in the lower latitudes east of the trough there was a continual flow of air toward lower contours.

Vertical motions were computed using the adiabatic assumption, $d\Theta/dt = 0$ or

$$w = \frac{-\left(\frac{\partial \Theta}{\partial t} + v_h \cdot \nabla_h \Theta\right)}{\frac{\partial \Theta}{\partial z}} + \left(\frac{\partial z}{\partial t}\right)_p, \quad (5)$$

where the subscript h indicates the horizontal component on a pressure surface, and the last term is the local change in height of the pressure surface. Since observational errors were quite large compared to gradients and time changes in this case, vertical motions were computed using mean values for the layer 500—300 mb. In this way, at least the larger temperature errors could be eliminated subjectively by using contour analyses at the two levels involved. Local values of wind

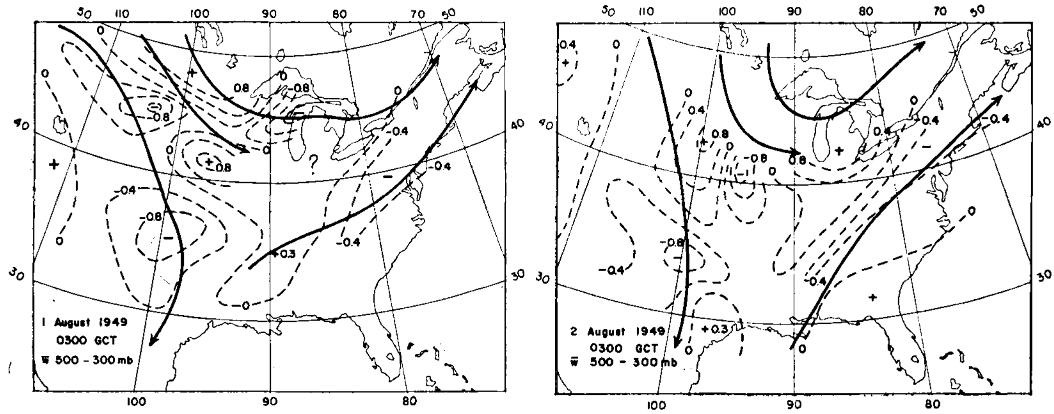

Fig. 11. Mean vertical motion (cm sec^{-1}) in layer 500—300 mb, corresponding to charts in fig. 10. Heavy arrows indicate axes of jet streams at 300 mb. Only values south of about latitude 40° are redarged as reliable.

velocity (weighted vector means of 20-, 25-, and 30,000-ft winds) were used in the computations, rather than finite-time trajectories. The results can only be taken as semi-quantitative owing to the assumption of adiabatic conditions, the difficulty of measuring gradients exactly from maps, and the fact that strictly equation (5) cannot be applied to mean values of quantities which may have irregular distributions through the layer concerned.

Figure 11 shows the computed vertical velocities (the irregular pattern north of about latitude 40° is not reliable). Between latitudes 30° and 40°, there is on the average across the whole trough region a weak descent of around 0.3 cm sec^{-1} (300 m per day). Thus considering the trough as a whole in relation to its environment, there is a weak vertical circulation in a direct solenoidal sense, in agreement with the usual observation in outbreaks of cold air (7, 19, 21). Assuming a minimum of vertical motion somewhere near the tropopause, there must be on the average a weak vertical stretching in the higher troposphere which should contribute to a slow increase of vorticity in the trough region through horizontal convergence.

The regions of maximum descent are located, not in the central part of the trough, but near the jet streams (the same distribution was observed at 1500 GCT 1 and 2 August). This is probably significant in understanding the maintenance of approximate balance between the changing vorticity field in the upper levels, and the temperature field. Leaving aside horizontal advective processes (which strictly cannot be neglected), a subsidence of the cold air reaching maximum value in the central part of the trough would tend to weaken the thermal gradient across the jets bounding it. Such a change in the thermal structure would in general be incompatible with increasing vorticity in the higher levels, which as discussed above would be a product of the lower-level subsidence. This apparent inconsistency is obviated if the vertical motions are distributed as in fig. 11. Here, although there is a mean subsidence in the trough region, the vertical motions are so distributed as to contribute to an increase in the thermal vorticity in the central part of the trough.

General conclusions — The above analysis indicates that in understanding the mechanism of generation and redistribution of winds in the free atmosphere, it is necessary to consider those terms in the vorticity relationships involving differential vertical motions and the variations of the nongeostrophic wind with height. Although this conclusion is by no means new, it appears worth-while to emphasize it at this time when there is a great deal of interest in problems concerning the structure of the wind field, particularly in the vicinity of the jet stream. There appears to be no basic difficulty in accounting for the generation of high values of vorticity in some important regions of the atmosphere, although the particular region near the maximum-wind level defies understanding, so far as the writers are concerned.

A complete explanation of the vorticity distribution cannot be arrived at solely on the basis of latitudinal exchange of air carrying with it vorticity derived from the rotation of the earth's surface, or on the basis of horizontal convergence and divergence processes. Deviations from the distribution obtained by horizontal exchange processes are, however, chiefly to be expected in middle latitudes where horizontal variations of vertical motions (i.e. differential tilting) and agradient motions accompanying travelling cyclones and anticyclones are generally greatest. The larger-scale features of the planetary vorticity distribution must still be explainable mainly on the basis of horizontal exchange processes, as the mean gradient of vertical velocity from pole to equator is very small. The vorticity-exchange theory of ROSSBY (27, 29) is not incompatible with the observed fact that there may be several jet streams in middle latitudes, since that theory is not intended to explain the details but the planetary distribution of vorticity.

The above results might be compared with the "confluence theory" of the jet stream, proposed by NAMIAS and CLAPP (15). These authors recognize the need for a direct solenoidal circulation in the horizontal, in accounting for the generation of strong winds in the upper troposphere. This point has also been strongly emphasized by PALMÉN (18, 20), as a necessity for understanding the general circulation of the atmosphere. The difference between the circulation pattern outlined above (fig. 8) and that proposed by NAMIAS and CLAPP in the vicinity of a developing jet, is that the *vertical-motion* branch of the circulation must be in an indirect rather than a direct solenoidal sense, at least in the region of increasing individual vorticity. This is not incompatible with the subsidence of cold air, so long as that subsidence is properly distributed. Since horizontal motions are so much greater than those in the vertical, the net circulation involved in generation of strong upper winds must still be in a direct sense.

Although in this case the examples used were chiefly in the higher troposphere, the results are clearly applicable also to the middle troposphere, since the strongest vertical motions are found at the principal level of nondivergence, located on the average near 600 mb. Although the conversion of vorticity through differential vertical motions (whose importance is a function of the frame of reference used) would not be a factor in numerical forecasting models using potential temperature as a vertical coordinate, it is apparent that the lack of inclusion of this process in models using *xyz*-coordinates could lead to serious errors in the results obtained.

HOUGHTON and AUSTIN (10) and others have emphasized the importance of studying the non-gradient motions in connection with the mechanism of pressure changes and generation of kinetic energy. Since these motions cannot be computed but must be observed, it is clear that to obtain positive results in synoptic research the network of stations capable of observing winds to high levels under adverse conditions must be considerably increased. Otherwise, results are bound to be fragmentary and approximate. HOVMÖLLER (11) has recently demonstrated, in a very striking way, the difficulty of obtaining even a reliable first approximation to the wind field, from radiosonde data alone (although the subjective process of analysis improves the situation). A serious difficulty encountered in attempts to make a detailed analysis of the wind field is that the present wind code (at least in North America) provides reports only at 5,000-ft intervals above 20,000 ft. The usefulness of wind reports could be considerably augmented by the inclusion of "significant levels" as in the radiosonde code, that is, levels at which the vertical shear changes in a significant manner.

Acknowledgment — The writers are indebted to Prof. C.-G. ROSSBY for his generous guidance and stimulating discussions during the course of this work. Both Prof. ROSSBY and Prof. J. VAN MIEGHEM suggested that the effects of nonconservative processes on the vorticity field be investigated. We thank Fil. Lic. B. BOLIN and Prof. E. PALMÉN for critically reading the manuscript in semi-finished form, and making several very helpful suggestions for its improvement.

REFERENCES

1. BELLAMY, J. C., 1945: The use of pressure altitude and altimeter corrections in meteorology. *J. Meteor.*, 2, 1—79.
2. BERGGREN, R., 1952: The distribution of temperature and wind connected with active tropical air in the higher troposphere and some remarks concerning clear air turbulence at high altitude. *Tellus*, 4, 43—53.
3. BJERKNES, J., 1951: Extratropical cyclones. *Compendium of Meteorology*, Amer. Meteor. Soc., 577—598.
4. CRESSMAN, G. P., 1948: On the forecasting of long waves in the upper westerlies. *J. Meteor.*, 5, 44—57.
5. — 1950: Variations in the structure of the upper westerlies. *J. Meteor.*, 7, 39—47.
6. ERTEL, H., 1942: Ein neuer hydrodynamische Wirbelsatz. *Meteor. Zeit.*, 59, 277—281.
7. FLEAGLE, R. G., 1947: The fields of temperature, pressure, and three-dimensional motion in selected weather situations. *J. Meteor.*, 6, 165—185.
8. FUGLISTER, F. C., 1951: Multiple currents in the Gulf Stream System. *Tellus*, 3, 230—233.
9. GUSTAFSON, A. F., 1949: *Final report on the upper wind project*. Univ. Calif. at Los Angeles (mimeographed).
10. HOUGHTON, H. G., and AUSTIN, J. M., 1946: A study of non-geostrophic flow with applications to the mechanism of pressure changes. *J. Meteor.*, 3, 57—87.
11. HOVMÖLLER, E., 1952: A comparison between observed and computed winds with respect to their applicability for vorticity computations. *Tellus*, 4, 126—134.
12. HSIEH, Y.-P., 1950: On the formation of shear lines in the upper atmosphere. *J. Meteor.*, 7, 382—387.
13. MURRAY, R., and JOHNSON, D. H., 1952: Structure of the upper westerlies: a study of the wind field in the eastern Atlantic and western Europe in September 1950. *Quart. J. R. Met. Soc.*, 78, 186—199.
14. NAMIAS, J., and CLAPP, P. F., 1944: Studies of the motion and development of long waves in the westerlies. *J. Meteor.*, 1, 57—77.
15. — 1949: Confluence theory of the high tropospheric jet stream. *J. Meteor.*, 6, 330—336.
16. NEWTON, C. W., PHILLIPS, N. A., CARSON, J. E., and BRADBURY, D. L., 1951: Structure of shear lines near the tropopause in summer. *Tellus*, 3, 154—171.
17. PALMÉN, E., 1949: Origin and structure of high-level cyclones south of the maximum westerlies. *Tellus*, 1, No. 1, 22—31.
18. — 1949: Meridional circulations and the transfer of angular momentum in the atmosphere. *J. Meteor.*, 6, 429—430.
19. — 1951: The aerology of extratropical cyclones. *Compendium of Meteorology*, Amer. Meteor. Soc., 599—620.
20. — 1951: The role of atmospheric disturbances in the general circulation. *Quart. J. R. Met. Soc.*, 77, 337—354.
21. — and NEWTON, C. W., 1951: On the three-dimensional motions in an outbreak of polar air. *J. Meteor.*, 8, 25—39.
22. PHILLIPS, N. A., 1950: The behaviour of jet streams over eastern North America during January and February 1948. *Tellus*, 2, 116—124.
23. PLATZMAN, G. W., 1949: The motion of barotropic disturbances in the upper troposphere. *Tellus*, 1, No. 3, 53—64.
24. RIEHL, H., 1948: Jet stream in upper troposphere and cyclone formation. *Trans. Amer. geophys. Un.*, 29, 175—186.
25. — *and collaborators*, 1952: Forecasting in middle latitudes. *Meteor. Monographs*, 1, No. 5 (80 p.).
26. ROSSBY, C.-G., 1938: On the mutual adjustment of pressure and velocity distribution in certain simple current systems, II. *J. Mar. Res.*, 1, 239—263.
27. — 1947: On the distribution of angular velocity in gaseous envelopes under the influence of large scale horizontal mixing processes. *Bull. Amer. meteor. Soc.*, 28, 53—68.
28. SHERMAN, L., 1952: On the scalar-vorticity and horizontal-divergence equations. *J. Meteor.*, 9, 359—366.
29. UNIVERSITY OF CHICAGO, DEPARTMENT OF METEOROLOGY, 1947: On the general circulation of the atmosphere in middle latitudes. *Bull. Amer. meteor. Soc.*, 28, 255—280.
30. VAN MIEGHEM, J., 1950: Sur la circulation transversale associée à un courant atmosphérique. *Tellus*, 2, 52—55.